The rate-limiting step for photosynthetic CO_2 utilization under varying atmospheric evaporative demand in *Solanum lycopersicum* (tomato)

Dalong Zhang
Northwest Agriculture and Forestry University
Qingming Li
Shandong Agricultural University
Wataru Yamori
The University of Tokyo
Min Wei (minwei1968@163.com)

Research article

Keywords: Vapour pressure deficit; Photosynthetic limitation, Stomatal conductance, Mesophyll conductance, Water transport, Tomato

Posted Date: January 10th, 2020

DOI: https://doi.org/10.21203/rs.2.20548/v1

Abstract

Background: Despite atmospheric vapour pressure deficit (VPD) was demonstrated as significant environmental factors affecting plant photosynthesis and productivity, the regulating mechanism under varying atmospheric evaporative demand was still unclarified. The contribution of stomatal, mesophyll resistance and biochemical limitation imposed on photosynthesis in tomato under varying evaporative demand was highlighted in the present study. Quantitative photosynthetic limitation analysis across a series of VPD was performed in well-watered tomato, by combining gas exchange and chlorophyll fluorescence.

Results: Photosynthetic performance in tomato was gradually depressed with increasing in VPD. Under low VPD condition, stomatal and mesophyll conductance were sufficiently high for CO_2 transport, which facilitated high chloroplast CO_2 concentration for carbon fixation. Stomatal and mesophyll limitation accounted a low fraction, and photosynthetic potential was mostly constrained by biochemical limitation inside chloroplasts under low VPD condition. With increasing in VPD, plant water stress was gradually pronounced and triggered declines in stomatal and mesophyll conductance. Contribution of stomatal and mesophyll limitation on photosynthesis increased gradually with rise in VPD. Consequently, the low CO_2 availability inside chloroplast substantially constrained photosynthesis under high VPD condition.

Conclusion: Photosynthetic potential in tomato was mostly constrained by biochemical limitation inside chloroplasts under low VPD condition. CO_2 diffusion limitation in series of stomatal and mesophyll resistance was the key rate-limiting step for photosynthesis under high VPD condition.

Background

CO_2 is fundamental for maximum the potentials in photosynthetic rate, plant growth and yield. CO_2 elevation improves plant growth and increases yield via enhancing photosynthesis. Elevated atmospheric carbon dioxide concentration ($[CO_2]$) is a major component of climate change [1]. The global atmospheric CO_2 concentration has increased from 280 μmol mol^{-1} during the pre-industrial period to 395 μmol mol^{-1} in 2014 (http://www.esrl.noaa.gov/). It is predicted that the CO_2 concentration will rise globally to 550 μmol mol^{-1} in the middle of the present century, and increase to 700 ~ 900 μmol mol^{-1} by the end of the 21^{st} century [2, 3]. In addition, the greenhouse industry facilitated CO_2 fertilization to enhance plant growth and productivity in the semi-closed ecosystem, which was widely applied throughout the word to improve crop productivity. Although CO_2 fertilization and the globally elevated trends are expected to improve crop photosynthesis and increase yield, large evidence was provided that the magnitude of such enhancement is constrained by other climate change derived phenomena, such as the more extreme and more frequent environmental stress [4]. The bottlenecks constraining CO_2 utilization efficiency is the limited plant photosynthetic capacity for CO_2 acquisition and assimilation.

Photosynthetic CO_2 uptake and transport is constrained by a series of resistance, which was simplified into stomatal and mesophyll resistance [5]. Guard cells of stomata are first “barrier” for gas exchange, which restrict photosynthetic CO_2 uptake and transpiration [6]. In additional to stomatal resistance, large evidences were provided that CO_2 movement from sub-stomatal cavity to carbon fixation site is constrained by the great mesophyll resistance, which substantially depress photosynthesis rate, especially for C_3 plant [7–12]. Environmental fluctuation is thought to profoundly affect CO_2 uptake and transport. Large evidences were provided that stomatal and mesophyll conductance respond rapidly and sensitively to the external environmental variation [12–14]. It has been recognized that CO_2 movement and carbon fixation is regulated by environmental factors such as soil moisture [15, 16], light [17], temperature [18, 19] and so on.

Among of these environmental stimulate, effect of atmospheric evaporative demand on photosynthetic CO_2 uptake and transport received far less attention. From a physics perspective, atmospheric vapour pressure deficit (VPD) is evaporative driving force for water transport at leaf-atmospheric boundary [20]. Previous study demonstrated that VPD regulation profoundly affect plant water status, photosynthetic performance and yield production [21–23]. The increasing sophistication of the greenhouse industry facilitates precise atmospheric VPD regulation [24, 25]. Despite VPD was an important environmental factor which significantly affect photosynthetic performance, few previous studies have quantitatively addressed the components of photosynthetic limitation under contrasting VPD condition. The rate-limiting step for photosynthetic CO_2 transport and utilization under varying VPD was highly uncertain. A quantitative limitation analysis consisting of stomatal, mesophyll and biochemical limitations was essential to reveal the underlying mechanism of VPD regulating photosynthetic process.

The present study was aimed to identify the rate-limiting process for photosynthetic CO_2 uptake and fixation under varying atmospheric evaporative demand in C_3 plant tomato, by addressing three questions: (1) Which was the most significant limitation for photosynthesis under varying VPD condition. (2) How did diffusion conductance comparing stomatal and mesophyll conductance tuned with VPD. (3) How did the contribution of stomatal and mesophyll limitation on photosynthesis varied with VPD. In the present study, well-irrigated tomato plants were grown under contrasting VPD condition, in controlled-environment greenhouse.

Results

Effect of VPD on water transport forces along soil-plant-atmospheric continuum

VPD significantly affected the distribution of water free energy along soil-plant-atmospheric pathway, as illustrated in Fig. 1. Atmospheric evaporative demand increased with the rise in VPD, which triggered plant water stress and the linear declines in leaf water potential (Fig. 1A). With rise in VPD, the drawdown of Ψ_{leaf} in high-VPD grown plants was slighter than low-VPD treatment plants, according to the slope of linear regression (Fig. 1A). The driving force for passive water flow between soil and leaf ($\Delta\Psi_{soil\text{-}leaf}$)

increased with VPD, and the magnitude of increment was greater in low-VPD grown plants than high-VPD plants (Fig. 1B). Since Ψ_{leaf} was negligible compared with the large air negative potential, water driving force at leaf-air boundary ($\Delta\Psi_{leaf\text{-}air}$) increased dramatically with rise in VPD, with minor difference among treatments (Fig. 1C). The magnitude for increment in $\Delta\Psi_{leaf\text{-}air}$ was considerably greater than $\Delta\Psi_{soil\text{-}leaf}$, and the difference between $\Delta\Psi_{leaf\text{-}air}$ and $\Delta\Psi_{soil\text{-}leaf}$ was enlarged with VPD. The ratio of $\Delta\Psi_{leaf\text{-}air}$ to $\Delta\Psi_{soil\text{-}leaf}$ increased logarithmically from approximately 50 at 0.5 KPa to 150 at 1.5 KPa, and then maintained at a steady level (Fig.1D).

Effect of VPD on photosynthetic parameters of tomato

Photosynthesis rate responded to CO_2 elevation in similar patterns regardless of cultivars and growth VPD condition: photosynthesis rate rise rapidly across low CO_2 concentration and then reached a steady-state (Fig.S1). However, the maximum steady-state of photosynthesis rate declined with VPD increased from 0.5 to 4.5 KPa (Fig.S1). Maximum carboxylation rate (V_{cmax}), maximum electron transport rate (J_{max}) and carboxylation efficiency (CE) declined linearly with rise in VPD (Fig. 2). The drawdown of V_{cmax}, J_{max} and CE with rise in VPD was moderated in high-grown plants than low-VPD grown plants, according to the slope of linear regression (Fig. 2).

Effect of VPD on photosynthetic CO_2 uptake and transport

Stomatal, mesophyll and total conductance for CO_2 diffusion decreased linearly with increasing VPD, regardless of cultivars and growth VPD condition (Fig. 3). The magnitudes of drawdown in stomatal, mesophyll and total conductance were slighter in high-VPD grown plants than low-VPD grown plants, for both two cultivars (Fig. 3).

The CO_2 concentration of intercellular and chloroplast along the “source-path-sink” was reduced by different extent with rise in VPD (Fig. 4A, B). The drawdowns of C_i and C_c caused by VPD elevation was relative lower in high-VPD grown plants, compared with low-VPD plants (Fig. 4C, D, E). Consequently, the ratio of C_i/C_a, C_c/C_a and C_c/C_i linearly decreased with rise in VPD. The declining slope of C_i/C_a, C_c/C_a and C_c/C_i versus VPD was lower in high VPD grown plants, compared with low-VPD plants (Fig. 4C, D, E).

Partial photosynthetic limitation

The fractions of stomatal, mesophyll and biochemical limitation imposed on photosynthesis were not constant, which varied with the rise in VPD (Fig. 5). Under low VPD condition, stomatal and mesophyll conductance for CO_2 diffusion was high and imposed minor limitations on photosynthesis. Stomatal and mesophyll conductance accounted for a low proportion of photosynthetic limitation, while biochemical carboxylation for carbon fixation was the most significant limitation for photosynthetic process under low VPD condition (Fig. 5A, B, C). The fraction of total limitations attributed to stomatal limitation increased linearly with VPD, from approximately 15% at 0.5 KPa to 35% at 4.5 KPa (Fig. 5A). Similar pattern was observed in mesophyll limitation: The fraction of total limitations attributed to stomatal

limitation also increased linearly with VPD, from approximately 23% at 0.5 KPa to 33% at 4.5 KPa (Fig. 5B). The increments in the fractions of stomatal and mesophyll limitation tended to less marked in high VPD grown plants. In contrast, fraction of total limitations attributed to biochemical limitation of carbon fixation gradually linearly decreased with increasing VPD, from approximately 65% at 0.5 KPa to 35% at 4.5KPa (Fig. 5C).

Thereby, biochemical limitation was most significant limitation and rate-limiting step for photosynthetic process under low VPD condition, regardless of cultivars and growth VPD condition (Fig. 6). The constrains of stomatal and mesophyll limitation imposed on photosynthesis gradually increased and predominated with increasing VPD (Fig. 6). Under high VPD condition, diffusion conductance of stomatal and mesophyll imposed the greatest limitation for photosynthesis in tomato, which were the rate-limiting step for photosynthetic process (Fig. 6).

Correlations among g_m, g_s, leaf water status and LMA

Leaf mesophyll conductance was significantly and positively correlated with stomatal conductance (Fig. 7A). Meanwhile, stomatal and mesophyll conductance for CO_2 diffusion was closely linked to leaf water status: significant and positive correlations were found in leaf water potential versus stomatal and mesophyll conductance (Fig.7B, C). Acclimation to contrasting VPD condition modified leaf structural traits: LMA tended to be increased in high-VPD grown plants, compared with low-VPD plants (Fig. S2A). A significant and negative correlation between g_m versus LMA was observed (Fig. S2B).

Discussion

The present study demonstrated that photosynthetic performance in tomato was significantly affected by the atmospheric evaporative demand. The proportion of individual limitation components including stomatal conductance, mesophyll conductance and biochemical carboxylation inside chloroplast were not constant with varying VPD. The relative contribution of stomatal, mesophyll resistance and biochemical carboxylation imposed on photosynthesis varied under contrasting VPD condition. Thereby, the key rate-limiting step for photosynthetic performance varied with rise in VPD: under low VPD condition, stomatal and mesophyll conductance was sufficiently high for efficiently CO_2 transport, which facilitated high CO_2 availability inside chloroplast for carbon fixation; diffusion limitation of stomatal and mesophyll conductance accounted for a low fraction of total photosynthetic limitation under low VPD condition, biochemical carboxylation was the key rate-limiting step for raising photosynthetic potential of tomato. With VPD increasing, stomatal and mesophyll conductance for CO_2 transport declined. Stomatal and mesophyll limitation on photosynthesis increased gradually with rise in VPD. Consequently, the low chloroplast CO_2 concentration substantially constrained photosynthesis under high VPD condition. Thereby, CO_2 diffusion limitation in series of stomatal and mesophyll resistance was key rate-limiting step for photosynthesis under high VPD condition.

Three steps were involved in the potential mechanism accounting for the increased significant limitation of stomatal and mesophyll conductance imposed on photosynthesis in tomato with rise in VPD, which was illustrated in Fig.6: (□) rise in VPD caused plant water stress via disrupting the mass balance between soil water supply and atmospheric evaporative demand. (□) plant water stress with rise in VPD triggered stomatal closure and reduced stomatal conductance for CO_2 uptake. (□) leaf anatomical acclimation to atmospheric drought modulated mesophyll conductance for CO_2 transport within leaf.

Rising in VPD triggered plant water stress via disrupting the mass balance between soil water supply and atmospheric evaporative demand

Passive water movement was driven by the gradually declined free energy along soil-plant-atmospheric continuum, which can be quantified as the gradient in water potential in liquid phase. Water movement at leaf-air boundary in gas phase was driven by the difference in VPD. Based on physical principles, excessive air desiccation triggered high VPD and great negative air water potential. $\Delta\psi_{leaf\text{-}air}$ was substantial greater than $\Delta\psi_{soil\text{-}leaf}$, which pulled water out of plant. The substantial difference between $\Delta\psi_{leaf\text{-}air}$ and $\Delta\psi_{soil\text{-}leaf}$ was logarithmically enlarged with rise in VPD. Quantitatively, the atmospheric driving force at leaf-air boundary can be more than a hundredfold larger than soil-leaf component under high VPD condition. The great asymmetric between atmospheric evaporative demand and soil water supply triggered disruption in water balance despite plants were well irrigated. Root water uptake and supply was inadequate to keep pace with the great atmospheric driving force under high VPD condition, which consequently triggered leaf dehydration and declines in water potential. Thereby, VPD was crucial external stimulations pulling water out of soil and affect water balance. VPD fluctuated dramatically over the diurnal course in crop production, especially for greenhouse cultivation. Soil moisture was relatively stable over short term, with a minor variation compared with atmospheric evaporative demand [26]. Plant-water relations was regulated to a greater extent by VPD, and to a less extent modulated by soil moisture. Similar as soil drought, VPD induced atmospheric drought and plant water stress was also important factors triggering depression in photosynthesis.

Plant water stress with rise in VPD triggered stomatal closure and reduced stomatal conductance for CO_2 uptake

Stomata was the “gatekeepers” for exchange of water vapour and CO_2. Guard cells surrounding the stomatal pore respond to perturbations of soil-plant-atmospheric hydraulic continuum, which was putatively transduced into stomatal movements by feedback and feedforward mechanisms [27-29]. Stomatal control of transpired water loss was critical for sustaining physiological processes, such as leaf water status and photosynthetic CO_2 uptake. It has been recognized that plant respond to drought by closing guard cells to reduce excessive water loss and prevent the development of water deficit in plant tissues [30]. In the present study, atmospheric driving force was an order of magnitude greater than water supply, which lead to a great symmetry between water supply and evaporative demand. The water supply-evaporative demand symmetry triggered declines in leaf water potential and stomatal closure. However, the mechanism of VPD-triggered stomatal closure was still uncertain, which was‘black box’ [31].

Some hypotheses hold that stomatal closure under high VPD condition was a passive process triggered by leaf dehydration and turgor loss. However, large evidences were provided that high-VPD triggered stomatal closure was probably more than a passive process [32]. Some proposed hypothesis hold that high-VPD triggered stomatal closure was an active process rather than passive, since the plant stress hormone of abscisic acid (ABA) was continuously produced and delivered with transpiration stream to guard cell [33, 34]. However, it is not clarified whether the ABA mediated active process also participated in VPD-induced stomatal regulation in tomato.

Despite stomatal closure prevented excess water loss to maintain physiological process by passive or active mechanisms, the closed “gatekeepers” simultaneously increased the stomatal resistance for photosynthetic CO_2 uptake from air to intercellular. Intercellular CO_2 concentration was gradually reduced with rise in VPD. Consequently, stomatal limitation imposed on photosynthesis increased with rise in VPD. The declines in leaf water potential and stomatal conductance with rise in VPD was less marked in high-VPD grown plants in this research. The distinct response to VPD may can be attribute to the physiological acclimation to growth condition. Long-term acclimation to high VPD condition enhanced water stress tolerant, which prevent the dramatic declines in leaf water potential, stomatal conductance and photosynthetic parameters when subjected to atmospheric drought.

Anatomical determination for mesophyll conductance of CO_2 transport within leaf under contrasting VPD condition

In additional to the first barrier of stomata, CO_2 transported from intercellular to carboxylation site was constrained by a comparable resistance with stomata. The present study demonstrated that mesophyll resistance was a significant component of diffusion resistance from air to Rubisco in tomato. A strong positive correlation between mesophyll and stomatal conductance was observed among treatments. Similar as stomatal conductance, mesophyll conductance of tomato was also linearly reduced with rise in VPD. Under low VPD condition, stomatal conductance in coupled with mesophyll conductance was sufficiently high for efficient CO_2 transport to carboxylation site within chloroplasts. High diffusion conductance in series of stomatal and mesophyll facilitated high chloroplast CO_2 concentration for carbon fixation. With rise in VPD, CO_2 concentration drawdown along “air- substomatal cavity-chloroplasts” was enlarged. Consequently, CO_2 concentration inside chloroplasts was substantially reduced under high VPD condition. Limitation of mesophyll conductance imposed on photosynthesis gradually dominated with rise in VPD.

Unlike the rapid and sensitive stomatal response to external environment, mesophyll conductance from substomatal cavity to carbon fixation site was determined to a large degree by leaf anatomical traits [35-39]. Leaf dry mass area (LMA) was a composite of underlying traits affecting mesophyll conductance, such as lamina thickness, mesophyll thickness, cell wall thickness, cell shape and bulk leaf density [35]. LMA determined the upper limit on mesophyll conductance. Meanwhile, LMA was closely linked to abiotic stress tolerance [40, 41]. Generally, higher LMA was a good indicator of greater stress tolerant. In the present study, LMA of high-VPD grown plants was higher than low-VPD plants. Higher LMA of tomato

was an ecological strategy in response to atmospheric drought under high VPD condition. As aforementioned, root water uptake and supply were inadequate to keep pace with the great atmospheric driving force under high VPD condition. A higher LMA indicated dense structural traits, which buffered cellular transpired water loss and prevent leaf tissue dehydration under high VPD condition. However, CO_2 and water transport shared pathway through the mesophyll cell walls and perhaps plasma membranes within leaves [42-45]. Despite the dense structural traits improved drought tolerance, the resistance for CO_2 diffusion through substomatal cavity to chloroplasts was simultaneously increased. LMA was negatively correlated with mesophyll conductance in the present study, which was consistent with previous studies [46].

Conclusions

Photosynthetic performance of tomato was gradually constrained with rise in atmospheric evaporative demand. The key rate-limiting step for photosynthetic performance varied with rise in VPD. Under low VPD condition, stomatal and mesophyll conductance was sufficiently high and increased CO_2 availability inside chloroplast for carbon fixation; diffusion limitation of stomatal and mesophyll conductance accounted for a low fraction of total photosynthetic limitation under low VPD condition, biochemical carboxylation was the key rate-limiting step for raising photosynthetic potential of tomato. With increasing in VPD, plant water stress was gradually pronounced and triggered linear declines in stomatal and mesophyll conductance. Contribution of stomatal and mesophyll limitation on photosynthesis increased gradually with rise in VPD. Consequently, the low CO_2 availability inside chloroplast substantially constrained photosynthesis under high VPD condition. Thereby, CO_2 diffusion limitation in series of stomatal and mesophyll resistance was the key rate-limiting step for photosynthesis under high VPD condition in tomato.

Methods

Plant materials and growth conditions

The experiment was conducted in two controlled-environment greenhouses in same characteristics (15m in length, 10m in width and 3.5m in height, North-South oriented) at Shandong Agriculture University under spring-summer climatic condition, from May to August 2018. Two tomato cultivars [22] (JinPeng NO.1, CV1 hereafter, JinPeng&Co., Ltd., China; FenGuan, CV2 hereafter, ZhongYa &Co., Ltd., China) with distinct VPD response were examined. Seeds were sown in plugs for germination and transplanted at four-leaf stage to 4.5L plastic pots, containing same amount of organic substrate and perlite mixture in a 3:1 proportion (v/v). Soil moisture was maintained around 90% field capacity according to a previous method [21]. Plants were periodically trimmed to maintain rapid vegetative growth throughout experiments. Plants were grown in two environmental-controlled greenhouses, maintained in same growth condition but contrasting VPD: high VPD was achieved in natural greenhouse environment, with VPD approximately 3~5KPa around midday; low VPD was maintained at ranges of 0.5~1.5 KPa by

humidification. A high-pressure micro-fog system was activated when VPD exceed the target values, as the characteristics of system were described detailly in a previous study [22].

The effects of VPD perturbations on leaf photosynthetic performance and plant water status were investigated about 50 days after treatments. 15 uniform plants from each treatment were selected as samples and transferred to the growth cabinets in the evening, prior to photosynthetic measurements. Light and temperature of growth cabinets were controlled steadily at normal level throughout the experiment.

Leaf gas exchange and chlorophyll fluorescence

Leaf gas exchange and chlorophyll fluorescence were measured simultaneously on healthy and expanded leaflets at same nodes, by a LI-6400 XT portable gas-exchange system equipped with a leaf chamber fluorometer (LI-6400-40, Li-Cor, Inc., Lincoln, NE, USA). The whole portable gas-exchange system was enclosed in growth cabinets. VPD of growth cabinets and leaf chamber was simultaneously controlled across a series VPD of 0.5, 1.5, 2.5, 3.5 and 4.5KPa. The temperature, light and CO_2 concentration were controlled at a constant and steady condition throughout the experiment: temperature of 30±1°C; a saturating photosynthetic photon flux density (PPFD) of 1000 μmol m^{-2} s^{-1}; CO_2 concentration of 400 μmol mol^{-1}. VPD was increased stepwise across the gradients for at least 60 min, until photosynthesis and plant water status reached a new steady state.

The curve of photosynthesis rate (P_n) versus intercellular CO_2 concentration (C_i) was performed using a previous procedure[12], under a series VPD of 0.5, 1.5, 2.5, 3.5 and 4.5KPa. Briefly, P_n-C_i curve was performed by controlling the ambient CO_2 concentration (C_a) from 400 to 300, 200, 150, 100 and 50μmol mol^{-1}, and then increased to 400μmol mol^{-1}. After re-achieving a steady-state at 400μmol mol^{-1}, C_a was increased gradually from 400μmol mol^{-1} to 1200μmol mol^{-1}. Carboxylation efficiency (CE) was estimated according to linear regression of the P_n-C_i curve at the ranges of $C_a \leq$ 200μmol mol^{-1} [47]. The maximum rate Rubisco carboxylation capacity (V_{cmax}) and maximal rate of electron transport (J_{max}) were determined according to the FvCB model [48].

Estimation of photosynthetic CO_2 diffusion conductance

A simplified network[12] for CO_2 diffusion via “source-path-sink” was shown in Fig. S3: CO_2 diffusion was constrained by the resistances of stomata and mesophyll in series circuit, driven by the CO_2 partial pressure gradient.

CO_2 diffusion conductance through guard cells of stomata (g_{sc}) was determined according to water diffusion conductance (g_{sw}), and the ratio between molecular diffusivities of water and CO_2 in gas [49]. Mesophyll conductance (g_m) was estimated by the variable J method [50]:

$$g_m = \frac{P_n}{C_i - \frac{\Gamma^*\left(J + 8\left(P_n + R_d\right)\right)}{J - 4\left(P_n + R_d\right)}} \quad (1)$$

Where P_n was the net photosynthesis rate, C_i was the intercellular CO_2 concentration. P_n and C_i was measured by steady-state gas exchange. R_d was the mitochondrial respiration rate in the light, and Γ* was CO_2 compensation point inside chloroplast. R_d and Γ* were calculated according to a previous study [51]. Briefly, P_n-C_i curves were measured at two light density(75 and 500 μmol m^{-2} s^{-1}) at CO_2 concentration of 30 to 120 μmol CO_2 mol^{-1} air. Γ* (x-axis) and Rd (y-axis) was derived according to intersection point of P_n-C_i curves. J was the electron transport rate, were calculated as described by a previous study [52].

According to the series circuit, the total CO_2 diffusion resistance ($1/g_{tot}$) can be determined as [7]: $1/g_{tot} = 1/g_s + 1/g_m$. Therefore, g_{tot} can be determined as:

$$g_{tot} = \frac{1}{1/g_s + 1/g_m} \quad (4)$$

Partitioning of photosynthetic limitation

Photosynthetic limitation was divided into components of stomatal (L_s), mesophyll limitation (L_m) and biochemical limitation (L_m). The proportions of individual component imposed on photosynthesis was determined as[12] [35]:

$$L_s = \frac{g_{tot}/g_s \times \partial A/\partial C_c}{g_{tot} + \partial A/\partial C_c}$$
$$L_m = \frac{g_{tot}/g_m \times \partial A/\partial C_c}{g_{tot} + \partial A/\partial C_c}$$
$$L_b = \frac{g_{tot}}{g_{tot} + \partial A/\partial C_c} \quad (5)$$

By definition, $L_s + L_m + L_b = 1$; ∂A/∂C_c was determined as the slope of P_n-C_c curves at CO_2 concentrations of 40~110μmol mol^{-1}.

Determination of plant water status

Once photosynthetic measurements were completed, leaflets were harvested for determination of plant water status. Leaf water potential (ψ_{leaf}) was measured by a pressure chamber (PMS-1000, Corvallis, OR, USA). Some plants were kept in dark condition for about 8~10 h for the determination of soil water potential (Ψ_{soil}) [53]. Since water movement was approximate to zero under dark condition, and thereby Ψ_{soil} remained relative constant and can be assumed to equal the xylem pressure potential of leaf at dark condition.

Leaf morphology

After determination of photosynthesis and water status, leaflets area was measured by leaf area meter. The leaflets samples were dried at 80°C by oven to constant dry mass and weighted. Leaf mass area (LMA) was determined as the ratio of leaf dry mass to leaf area.

Abbreviations

VPD: Vapour pressure deficit; Ψ_{leaf}: leaf water potential; Ψ_{soil}: soil water potential; Ψ_{air}: air water; potential; $\Delta\Psi_{leaf\text{-}air}$: the drawdown of water potential between leaf and air; $\Delta\Psi_{soil\text{-}leaf}$: the drawdown of water potential between soil and leaf ; V_{cmax}: Maximum carboxylation rate ; J_{max}: maximum electron transport rate ; CE: carboxylation efficiency ; g_s: stomatal conductance ; g_m: mesophyll conductance ; g_{tot}: total conductance; C_a: ambient CO_2 concentration; C_i: CO_2 concentration of intercellular ; C_C: CO_2 concentration of carboxylation site inside chloroplast ; L_s: stomatal limitations imposed on photosynthesis rate; L_m: mesophyll limitations imposed on photosynthesis rate; L_b: biochemical limitations imposed on photosynthesis rate; LMA: leaf mass area; P_n: net photosynthesis rate; R_d: the rate of mitochondrial respiration in the light; Γ*: chloroplastic CO_2 compensation point

Declarations

Ethics approval and consent to participate

The authors declared that experimental research works on the plants described in this manuscript comply with institutional, national and international guidelines.

Consent for Publication

Not applicable

Availability of data and materials

All data generated or analyzed during this study are included in this published article and its supplementary information files.

Competing interests

The authors declare that they have no conflict of interest.

Funding

This project was supported by the Natural Science Foundation of Shandong Province (ZR2019BC035).

Authors' contributions

MW conceived and designed the experiments. QML and WY conducted the experiments. DLZ analyzed the data and wrote the manuscript. All authors reviewed and approved the manuscript.

Acknowledgement

Not applicable.

References

1. Fang L, Abdelhakim LOA, Hegelund JN, Li S, Liu J, Peng X, Li X, Wei Z, Liu F. ABA-mediated regulation of leaf and root hydraulic conductance in tomato grown at elevated CO_2 is associated with altered gene expression of aquaporins. Hortic. Res. 2019, 6(1):1-10.
2. Li X, Zhang G, Sun B, Zhang S, Zhang Y, Liao Y, Zhou Y, Xia X, Shi K, Yu J. Stimulated leaf dark respiration in tomato in an elevated carbon dioxide atmosphere. Sci.Rep. 2013, 3:3433.
3. Liu J, Hu T, Fang L, Peng X, Liu F. CO_2 elevation modulates the response of leaf gas exchange to progressive soil drying in tomato plants. Agric. For. Meteorol. 2019, 268:181-188.
4. Norby RJ. Plant water relations at elevated CO_2—implications for water-limited environments. Plant Cell Environ. 2002, 25(2):319-331.
5. Tholen D, Zhu XG. The mechanistic basis of internal conductance: a theoretical analysis of mesophyll cell photosynthesis and CO_2 diffusion. Plant Physiol. 2011, 156(1):90-105.
6. Lawson T, Blatt MR. Stomatal size, speed, and responsiveness impact on photosynthesis and water use efficiency. Plant Physiol. 2014, 164(4):1556-1570.
7. Niinemets U, Diaz-Espejo A, Flexas J, Galmes J, Warren CR. Role of mesophyll diffusion conductance in constraining potential photosynthetic productivity in the field. J. Exp. Bot. 2009, 60(8):2249-2270.
8. Flexas J, Barbour MM, Brendel O, Cabrera HM, Carriqui M, Diaz-Espejo A, Douthe C, Dreyer E, Ferrio JP, Gago J, et al. Mesophyll diffusion conductance to CO_2: an unappreciated central player in photosynthesis. Plant sci. 2012, 193-194:70-84.
9. Sharkey TD. Mesophyll conductance: constraint on carbon acquisition by C_3 plants. Plant Cell Environ. 2012, 35(11):1881-1883.
10. Kaldenhoff R. Mechanisms underlying CO_2 diffusion in leaves. Curr Opin Plant Biol. 2012, 15(3):276-281.
11. von Caemmerer S, Evans JR. Enhancing C_3 photosynthesis. Plant Physiol. 2010, 154(2):589-592.

12. Li Q, Wei M, Li Y, Feng G, Wang Y, Li S, Zhang D. Effects of soil moisture on water transport, photosynthetic carbon gain and water use efficiency in tomato are influenced by evaporative demand. Agric. Water Manage. 2019, 226:105818.
13. Xiong D, Liu X, Liu L, Douthe C, Li Y, Peng S, Huang J. Rapid responses of mesophyll conductance to changes of CO_2 concentration, temperature and irradiance are affected by N supplements in rice. Plant Cell Environ.2015, 38(12):2541-2550.
14. Li Q, Liu Y, Tian S, Liang Z, Li S, Li Y, Wei M, Zhang D. Effect of supplemental lighting on water transport, photosynthetic carbon gain and water use efficiency in greenhouse tomato. Sci. Hortic. 2019, 256:108630.
15. Pazzagli PT, Weiner J, Liu F: Effects of CO_2 elevation and irrigation regimes on leaf gas exchange, plant water relations, and water use efficiency of two tomato cultivars. Agric. Water Manage. 2016, 169:26-33.
16. Wang X, Du T, Huang J, Peng S, Xiong D. Leaf hydraulic vulnerability triggers the decline in stomatal and mesophyll conductance during drought in rice. J. Exp. Bot. 2018, 69(16):4033-4045.
17. Soares AS, Driscoll SP, Olmos E, Harbinson J, Arrabaca MC, Foyer CH. Adaxial/abaxial specification in the regulation of photosynthesis and stomatal opening with respect to light orientation and growth with CO_2 enrichment in the C_4 species Paspalum dilatatum. New Phytol.2008, 177(1):186-198.
18. Yamori W, Noguchi K, Hanba YT, Terashima I. Effects of internal conductance on the temperature dependence of the photosynthetic rate in spinach leaves from contrasting growth temperatures. Plant Cell Physiol. 2006, 47(8):1069-1080.
19. Bernacchi CJ, Portis AR, Nakano H, von Caemmerer S, Long SP. Temperature response of mesophyll conductance: implications for the determination of Rubisco enzyme kinetics and for limitations to photosynthesis in vivo. Plant Physiol. 2002, 130(4):1992-1998.
20. Fricke W. Water transport and energy. Plant Cell Environ. 2017, 40(6):977-994.
21. Zhang D, Du Q, Zhang Z, Jiao X, Song X, Li J. Vapour pressure deficit control in relation to water transport and water productivity in greenhouse tomato production during summer. Sci Rep. 2017, 7:43461.
22. Zhang D, Jiao X, Du Q, Song X, Li J. Reducing the excessive evaporative demand improved photosynthesis capacity at low costs of irrigation via regulating water driving force and moderating plant water stress of two tomato cultivars. Agric. Water Manage. 2018, 199:22-33.
23. Zhang D, Liu Y, Li Y, Qin L, Li J, Xu F. Reducing the excessive evaporative demand improved the water-use efficiency of greenhouse cucumber by regulating the trade-off between irrigation demand and plant productivity. HortScience. 2018, 53(12):1784-1790.
24. Lu N, Nukaya T, Kamimura T, Zhang D, Kurimoto I, Takagaki M, Maruo T, Kozai T, Yamori W. Control of vapor pressure deficit (VPD) in greenhouse enhanced tomato growth and productivity during the winter season. Sci. Hortic. 2015, 197:17-23.

25. Zhang D, Zhang Z, Li J, Chang Y, Du Q, Pan T. Regulation of vapor pressure deficit by greenhouse micro-fog systems improved growth and productivity of tomato via enhancing photosynthesis during summer season. *PloS one* 2015, 10(7):e0133919.
26. Caldeira CF, Bosio M, Parent B, Jeanguenin L, Chaumont F, Tardieu F. A hydraulic model is compatible with rapid changes in leaf elongation under fluctuating evaporative demand and soil water status. Plant Physiol. 2014, 164(4):1718-1730.
27. Buckley TN. How do stomata respond to water status? New Phytol. 2019.
28. Buckley TN. Modeling stomatal conductance. Plant Physiol. 2017, 174(2):572-582.
29. Buckley TN. The control of stomata by water balance. New Phytol.2005, 168(2):275-292.
30. Novick KA, Miniat CF, Vose JM. Drought limitations to leaf-level gas exchange: results from a model linking stomatal optimization and cohesion-tension theory. Plant Cell Environ. 2016, 39(3):583-596.
31. Buckley TN. Stomatal responses to humidity: has the 'black box' finally been opened? Plant Cell Environ. 2016, 39(3):482-484.
32. Pantin F, Blatt MR. Stomatal response to humidity: blurring the boundary between active and passive movement. Plant Physiol. 2018, 176(1):485-488.
33. Merilo E, Yarmolinsky D, Jalakas P, Parik H, Tulva I, Rasulov B, Kilk K, Kollist H. Stomatal VPD response: there is more to the story than ABA. Plant Physiol. 2018, 176(1):851-864.
34. Qiu C, Ethier G, Pepin S, Dube P, Desjardins Y, Gosselin A. Persistent negative temperature response of mesophyll conductance in red raspberry (*Rubus idaeus* L.) leaves under both high and low vapour pressure deficits: a role for abscisic acid? Plant Cell Environ. 2017, 40(9):1940-1959.
35. Muir CD, Hangarter RP, Moyle LC, Davis PA. Morphological and anatomical determinants of mesophyll conductance in wild relatives of tomato (*Solanum* sect. *Lycopersicon*, sect. *Lycopersicoides; Solanaceae*). Plant Cell Environ. 2014, 37(6):1415-1426.
36. Han J, Lei Z, Flexas J, Zhang Y, Carriqui M, Zhang W, Zhang Y. Mesophyll conductance in cotton bracts: anatomically determined internal CO_2 diffusion constraints on photosynthesis. J. Exp. Bot. 2018, 69(22):5433-5443.
37. Xiong D, Flexas J, Yu T, Peng S, Huang J. Leaf anatomy mediates coordination of leaf hydraulic conductance and mesophyll conductance to CO_2 in *Oryza*. New Phytol.2017, 213(2):572-583.
38. Carriqui M, Roig-Oliver M, Brodribb TJ, Coopman R, Gill W, Mark K, Niinemets U, Perera-Castro AV, Ribas-Carbo M, Sack L *et al*. Anatomical constraints to nonstomatal diffusion conductance and photosynthesis in lycophytes and bryophytes. New Phytol. 2019, 222(3): 1256-1270.
39. Earles JM, Theroux-Rancourt G, Roddy AB, Gilbert ME, McElrone AJ, Brodersen CR. Beyond porosity: 3D leaf intercellular airspace traits that impact mesophyll conductance. Plant Physiol. 2018, 178(1):148-162.
40. Xiong D, Flexas J. Leaf economics spectrum in rice: leaf anatomical, biochemical, and physiological trait trade-offs. J. Exp. Bot. 2018, 69(22):5599-5609.

41. Xiong D, Douthe C, Flexas J. Differential coordination of stomatal conductance, mesophyll conductance, and leaf hydraulic conductance in response to changing light across species. Plant Cell Environ. 2018, 41(2):436-450.
42. Barbour MM. Understanding regulation of leaf internal carbon and water transport using online stable isotope techniques. New Phytol. 2017, 213(1):83-88.
43. Drake PL, Boer HJD, Schymanski SJ, Veneklaas EJ. Two sides to every leaf: water and CO_2 transport in hypostomatous and amphistomatous leaves. New Phytol.2019. 222(3): 1179-1187.
44. Zhao M, Tan HT, Scharwies J, Levin K, Evans JR, Tyerman SD. Association between water and carbon dioxide transport in leaf plasma membranes: assessing the role of aquaporins. Plant Cell Environ. 2017, 40(6):789-801.
45. Groszmann M, Osborn HL, Evans JR. Carbon dioxide and water transport through plant aquaporins. Plant Cell Environ. 2017, 40(6):938-961.
46. Hassiotou F, Ludwig M, Renton M, Veneklaas EJ, Evans JR. Influence of leaf dry mass per area, CO_2, and irradiance on mesophyll conductance in sclerophylls. J. Exp. Bot. 2009, 60(8):2303-2314.
47. Sun J, Ye M, Peng S, Li Y. Nitrogen can improve the rapid response of photosynthesis to changing irradiance in rice (*Oryza sativa* L.) plants. Sci Rep. 2016, 6:31305.
48. Farquhar GD, von Caemmerer S, Berry JA. A biochemical model of photosynthetic CO_2 assimilation in leaves of C_3 species. Planta. 1980, 149(1):78-90.
49. Giuliani R, Koteyeva N, Voznesenskaya E, Evans MA, Cousins AB, Edwards GE. Coordination of leaf photosynthesis, transpiration, and structural traits in rice and wild relatives (*Genus* Oryza). Plant Physiol. 2013, 162(3):1632-1651.
50. Harley PC, Loreto F, Di Marco G, Sharkey TD. Theoretical considerations when estimating the mesophyll conductance to CO_2 flux by analysis of the response of photosynthesis to CO_2. Plant Physiol. 1992, 98(4):1429-1436.
51. Laisk A, Oja V. Dynamics of leaf photosynthesis. CSIRO Publishing, Melbourne, Australia 1998.
52. Tomas M, Flexas J, Copolovici L, Galmes J, Hallik L, Medrano H, Ribas-Carbo M, Tosens T, Vislap V, Niinemets U. Importance of leaf anatomy in determining mesophyll diffusion conductance to CO_2 across species: quantitative limitations and scaling up by models. J. Exp. Bot. 2013, 64(8):2269-2281.
53. Tsuda M, Tyree MT: Hydraulic conductance measured by the high pressure flow meter in crop plants. J. Exp. Bot. 2000, 51(345):823-828.

Supplementary Information

Fig.S1. Effect of VPD on photosynthetic CO2 response curves in two tomato cultivars grown under high- and low VPD condition. Values are means ± SE (n= 4~6 replicates).

Fig.S2. Effect of VPD on leaf mass area (A; LMA) and its correction with g_m (B).

Fig.S3. A simplified pathway for photosynthetic CO_2 uptake and transport. C_a, C_i and C_c represent the CO_2 concentration of air, intercellular and carboxylation site; g_s and g_m represent stomatal and mesophyll conductance for CO_2 diffusion, respectively; g_{tot} represent the total conductance summing stomatal and mesophyll resistance in series.

Figures

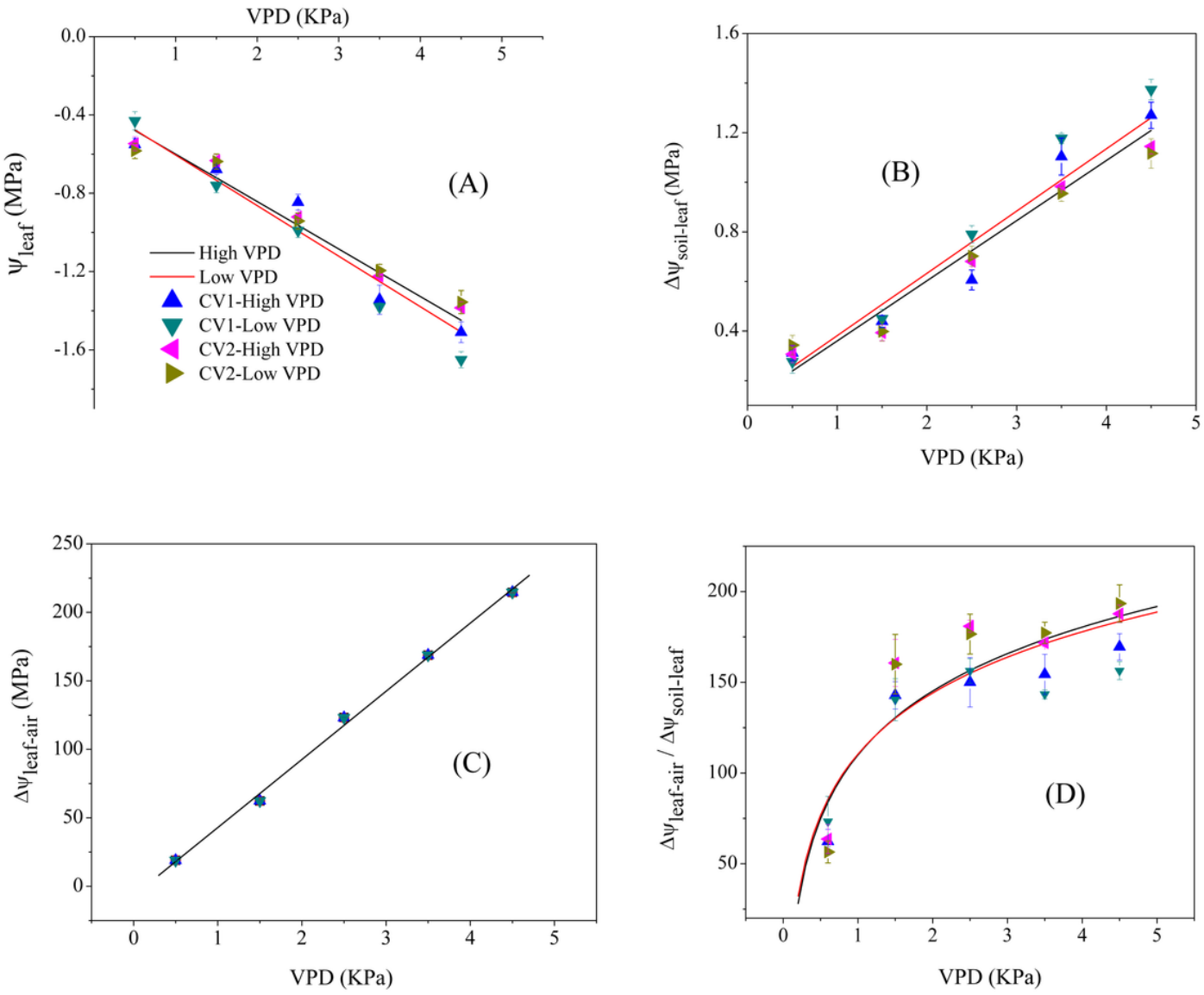

Figure 1

Effect of VPD on the spatial distribution of water potential and driving force (ΔΨ) between two spatial positions. Values are means ± SE (n= 4~6 replicates). The regression lines show are: (A) HVPD, Ψ leaf = -0.242VPD-0.358, R2=0.92; LVPD, Ψ leaf = -0.258VPD-0.347, R2=0.93. (B) HVPD, ΔΨsoil-leaf= 0.242VPD+0.118, R2=0.94; LVPD, ΔΨsoil-leaf = 0.251VPD+0.130, R2=0.93. (C) HVPD, ΔΨleaf-air =

49.8VPD-6.86, R2=0.98; LVPD, ΔΨleaf-air=49.8VPD-6.86, R2=0.98. (D) HVPD, ΔΨleaf-air/ΔΨsoil-leaf = 50.82ln(VPD)+109.95, R2=0.85; LVPD, ΔΨleaf-air/ΔΨsoil-leaf = 48.63ln(VPD)+110.41, R2=0.80.

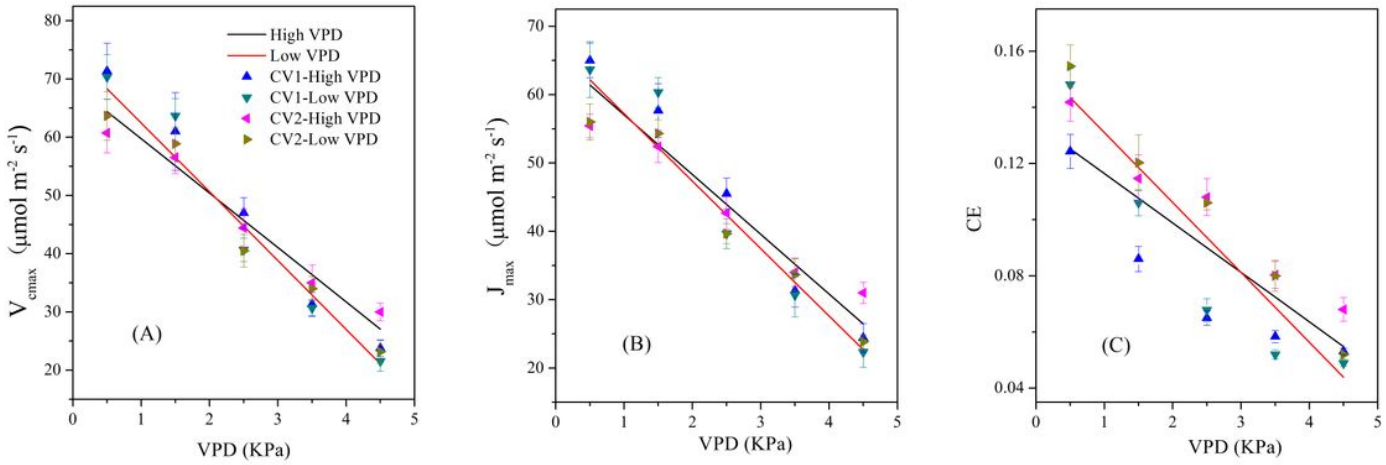

Figure 2

Effect of VPD on photosynthetic parameters of maximum rate Rubisco carboxylation capacity (Vcmax), maximal rate of electron transport (Jmax) and Carboxylation efficiency (CE). Values are means ± SE (n= 4 replicates). The regression lines show are: (A) HVPD, Vcmax= -10.39VPD+72.1, R2=0.95; LVPD, Vcmax= -11.82VPD+74.3, R2=0.95. (B) HVPD, Jmax= -8.74VPD+65.8, R2=0.93; LVPD, Jmax= -9.87VPD+67.1, R2=0.93. (C) HVPD, CE= -0.0176VPD+0.134, R2=0.74; LVPD, CE= -0.0249VPD+0.156, R2=0.88.

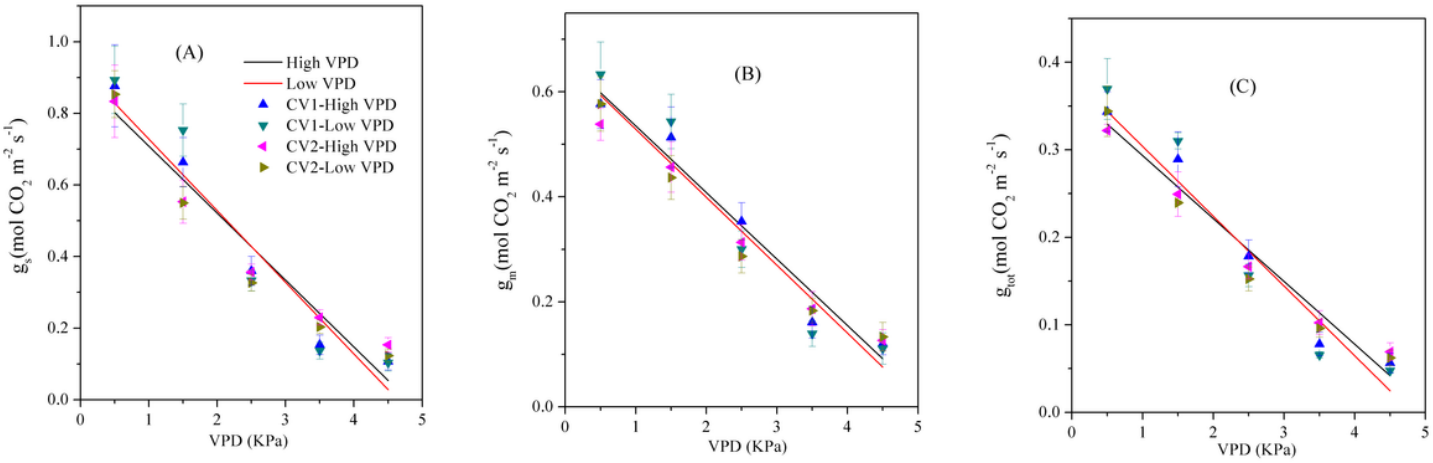

Figure 3

Effect of VPD on stomatal conductance (gs), mesophyll conductance (gm) and total conductance (gtot) for photosynthetic CO2 diffusion. Values are means ± SE (n= 4 replicates). The regression lines show are: (A) HVPD, gs= -0.187VPD+0.895, R2=0.94; LVPD, gs= -0.200VPD+0.928, R2=0.92. (B) HVPD, gm= -0.126VPD+0.661, R2=0.95; LVPD, gm= -0.129VPD+0.658, R2=0.94. (C) HVPD, gtot= -0.0719VPD+0.365, R2=0.95; LVPD, gtot= -0.0798VPD+0.384, R2=0.94.

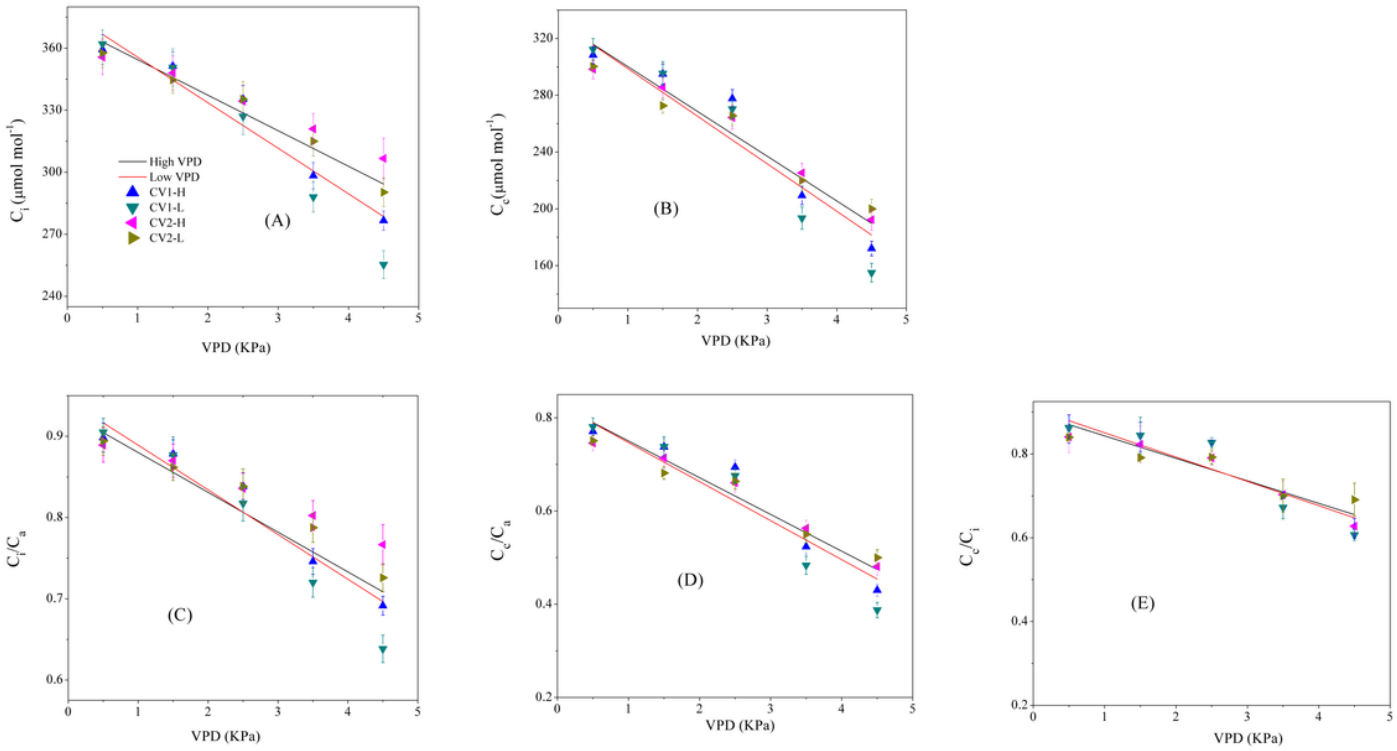

Figure 4

Effect of VPD on the CO2 concentration of intercellular (A; Ci), carboxylation site inside chloroplast (B; CC), and the ratio of intercellular to ambient CO2 concentration (C; Ci/Ca), the ratio of chloroplast to ambient CO2 concentration (D; Cc/Ca) and the ratio of chloroplast to intercellular CO2 concentration (E; Cc/Ci). The regression lines show are: (A) HVPD, Ci= -17.2VPD+371.6, R2=0.86; LVPD, Ci= -22.0VPD+377.6, R2=0.87. (B)HVPD, CC= -31.5VPD+331.6, R2=0.91; LVPD, CC= -33.5VPD+332.2, R2=0.88. (C) HVPD, Ci/Ca= -0.0429VPD+0.93, R2=0.86; LVPD, Ci/Ca= -0.055VPD+0.94, R2=0.87. (D) HVPD, Cc/Ca= -0.0788VPD+0.83, R2=0.92; LVPD, Cc/Ca= -0.0837VPD+0.83, R2=0.87. (E) HVPD, Cc/Ci= -0.0537VPD+0.89, R2=0.82; LVPD, Cc/Ci= -0.058VPD+0.91, R2=0.89.

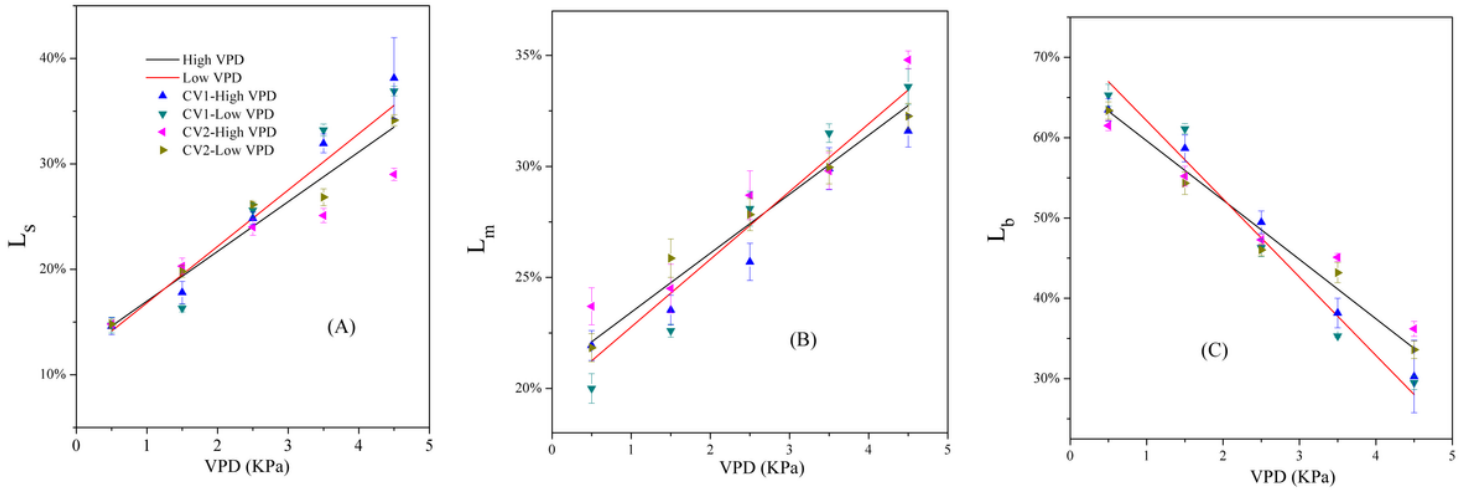

Figure 5

Quantitative limitations analysis comparing stomatal (A; Ls), mesophyll (B; Lm) and biochemical (C; Lb) limitations imposed on photosynthesis rate, under varying VPD. The regression lines show are: (A) HVPD, Ls= 0.0472VPD+0.122, R2=0.86; LVPD, Ls = 0.0535VPD+0.115, R2=0.89. (B) HVPD, Lm= 0.0266VPD+0.208, R2=0.88; LVPD, Lm = 0.0305VPD+0.197, R2=0.91.

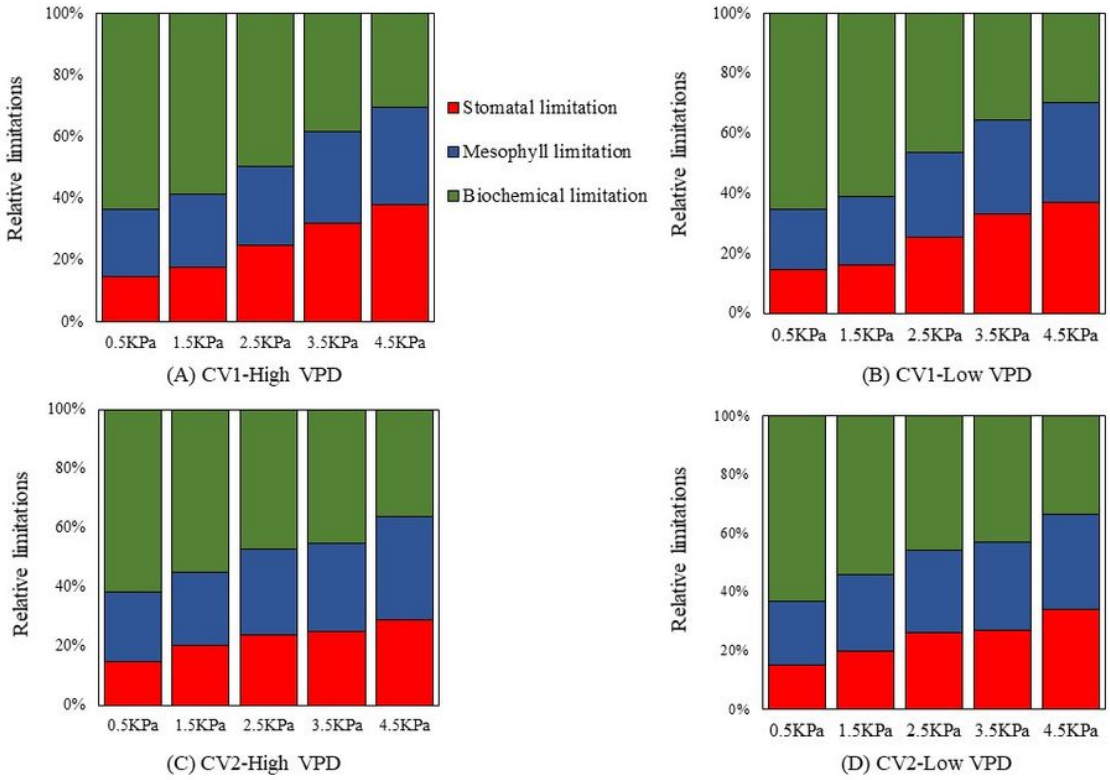

Figure 6

The dynamic change in the relative proportions of individual components of photosynthetic limitation under varying VPD.

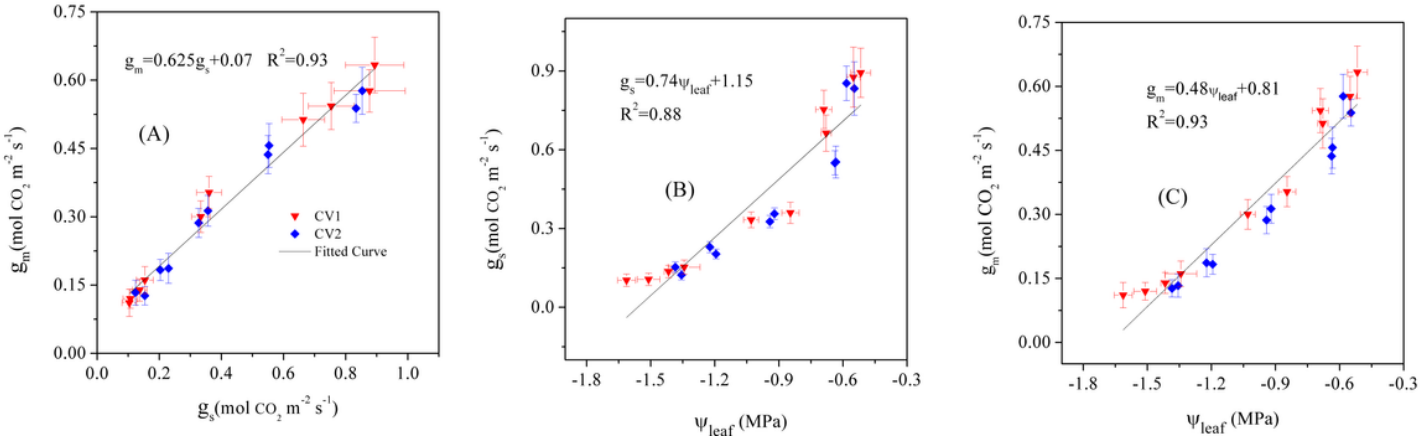

Figure 7

Correlations between gm versus gs (A), gs versus Ψ leaf (B), and gm versus Ψ leaf (C).

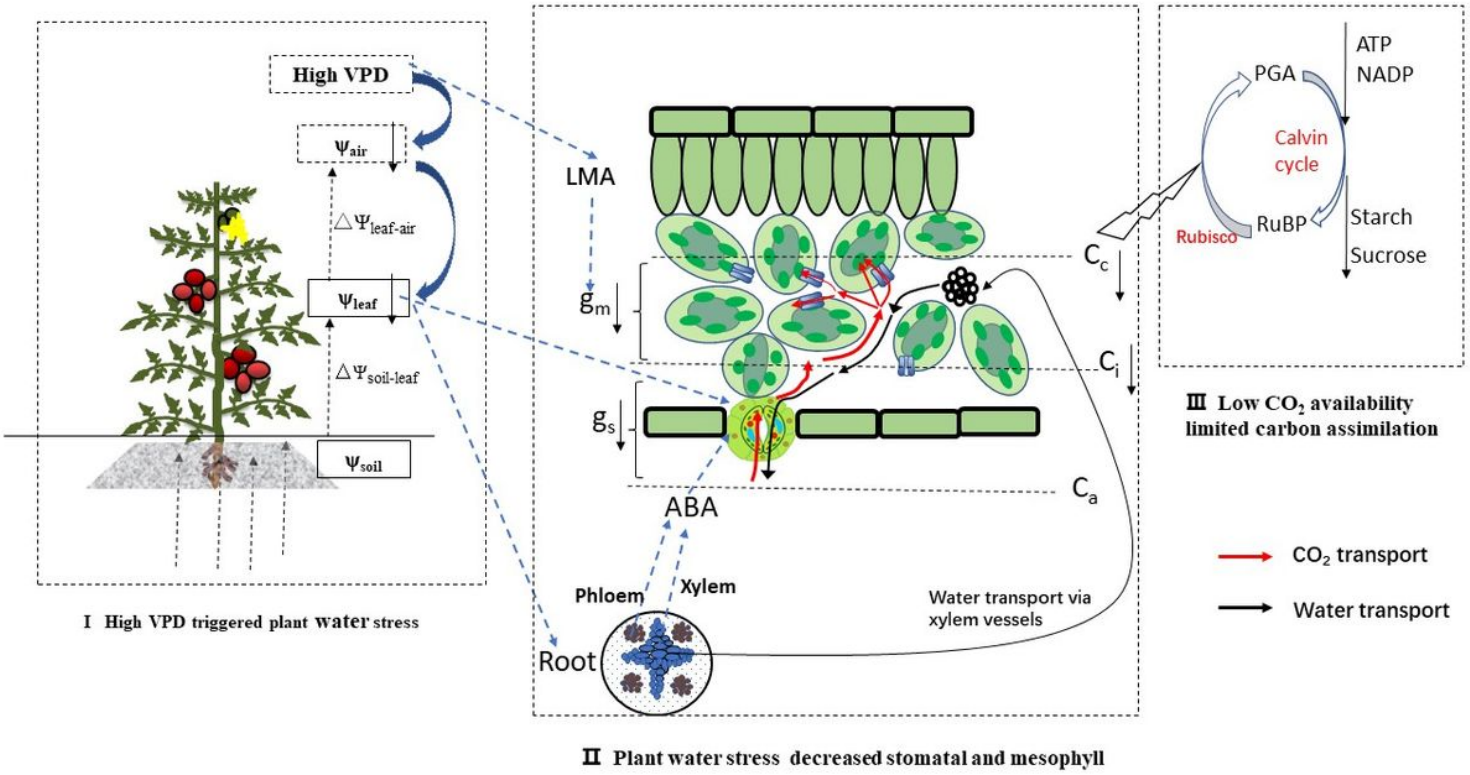

Figure 8

A potential schematic model accounting for the increased stomatal and mesophyll limitation on photosynthesis in tomato with rise in VPD: (□) rise in VPD caused plant water stress via disrupting the mass balance between soil water supply and atmospheric evaporative demand. (□) plant water stress with rise in VPD triggered stomatal closure and reduced stomatal conductance for CO2 uptake. (□) leaf anatomical acclimation to atmospheric drought modulated mesophyll conductance for CO2 transport within leaf.

Supplementary Files

This is a list of supplementary files associated with this preprint. Click to download.

- Supplementary.pdf